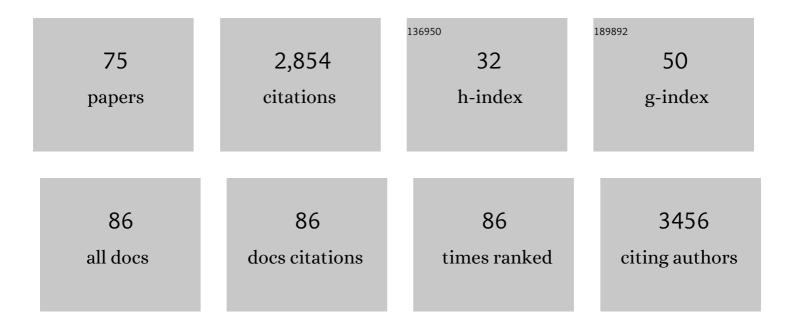
Alexei V Tivanski

List of Publications by Year in descending order

Source: https://exaly.com/author-pdf/3127161/publications.pdf Version: 2024-02-01



#	Article	IF	CITATIONS
1	The Sea Spray Chemistry and Particle Evolution study (SeaSCAPE): overview and experimental methods. Environmental Sciences: Processes and Impacts, 2022, 24, 290-315.	3.5	11
2	Size-Dependent Morphology, Composition, Phase State, and Water Uptake of Nascent Submicrometer Sea Spray Aerosols during a Phytoplankton Bloom. ACS Earth and Space Chemistry, 2022, 6, 116-130.	2.7	12
3	Nanomechanical variability in the early evolution of vertebrate dentition. Scientific Reports, 2022, 12, .	3.3	1
4	lsotopic Insights into Organic Composition Differences between Supermicron and Submicron Sea Spray Aerosol. Environmental Science & Technology, 2022, 56, 9947-9958.	10.0	4
5	Mechanical rigidity of a shape-memory metal–organic framework increases by crystal downsizing. Chemical Communications, 2021, 57, 89-92.	4.1	4
6	Mechanical cues protect against silica nanoparticle exposure in SH-SY5Y neuroblastoma. Toxicology in Vitro, 2021, 70, 105031.	2.4	4
7	Surface Tension Measurements of Aqueous Liquid–Air Interfaces Probed with Microscopic Indentation. Langmuir, 2021, 37, 2457-2465.	3.5	9
8	Atomic Force Microscopy: An Emerging Tool in Measuring the Phase State and Surface Tension of Individual Aerosol Particles. Annual Review of Physical Chemistry, 2021, 72, 235-252.	10.8	19
9	Probing the Water Uptake and Phase State of Individual Sucrose Nanoparticles Using Atomic Force Microscopy. ACS Earth and Space Chemistry, 2021, 5, 2612-2620.	2.7	6
10	Vanillin-bioglass cross-linked 3D porous chitosan scaffolds with strong osteopromotive and antibacterial abilities for bone tissue engineering. Carbohydrate Polymers, 2021, 271, 118440.	10.2	37
11	Fascin limits Myosin activity within Drosophila border cells to control substrate stiffness and promote migration. ELife, 2021, 10, .	6.0	25
12	Platelet-derived Growth Factor-α and Neuropilin-1 Mediate Lung Fibroblast Response to Rigid Collagen Fibers. American Journal of Respiratory Cell and Molecular Biology, 2020, 62, 454-465.	2.9	6
13	Semiconductor Cocrystals Based on Boron: Generated Electrical Response with π-Rich Aromatic Molecules. Crystal Growth and Design, 2020, 20, 3-8.	3.0	19
14	Physicochemical Mixing State of Sea Spray Aerosols: Morphologies Exhibit Size Dependence. ACS Earth and Space Chemistry, 2020, 4, 1604-1611.	2.7	18
15	Single Particle Atomic Force Microscopy. Microscopy and Microanalysis, 2020, 26, 3132-3132.	0.4	0
16	Mechanical Properties and Photomechanical Fatigue of Macro- and Nanodimensional Diarylethene Molecular Crystals. Nano Letters, 2020, 20, 6744-6749.	9.1	22
17	Phase State and Water Uptake Study of Individual Sea Spray Aerosol Particles Using Atomic Force Microscopy. Microscopy and Microanalysis, 2020, 26, 2500-2502.	0.4	0
18	Size Dependent Mechanical Properties and Photomechanical Fatigue of Diarylethene Molecular Crystals Using Atomic Force Microscopy. Microscopy and Microanalysis, 2020, 26, 2504-2505.	0.4	1

ALEXEI V TIVANSKI

#	Article	IF	CITATIONS
19	Rigid Double-Stranded DNA Linkers for Single Molecule Enzyme–Drug Interaction Measurements Using Molecular Recognition Force Spectroscopy. Langmuir, 2020, 36, 4174-4183.	3.5	8
20	Organic Enrichment, Physical Phase State, and Surface Tension Depression of Nascent Core–Shell Sea Spray Aerosols during Two Phytoplankton Blooms. ACS Earth and Space Chemistry, 2020, 4, 650-660.	2.7	29
21	A Soft Mechanical Phenotype of SH-SY5Y Neuroblastoma and Primary Human Neurons Is Resilient to Oligomeric Aβ(1–42) Injury. ACS Chemical Neuroscience, 2020, 11, 840-850.	3.5	16
22	Remarkable decrease in stiffness of aspirin crystals upon reducing crystal size to nanoscale dimensions <i>via</i> sonochemistry. CrystEngComm, 2019, 21, 2049-2052.	2.6	7
23	Size-Dependent Mechanical Properties of a Metal–Organic Framework: Increase in Flexibility of ZIF-8 by Crystal Downsizing. Nano Letters, 2019, 19, 6140-6143.	9.1	36
24	Correlating 3D Morphology, Phase State, and Viscoelastic Properties of Individual Substrate-Deposited Particles. Analytical Chemistry, 2019, 91, 7621-7630.	6.5	33
25	Effect of dry or wet substrate deposition on the organic volume fraction of core–shell aerosol particles. Atmospheric Measurement Techniques, 2019, 12, 2033-2042.	3.1	19
26	Saccharide Transfer to Sea Spray Aerosol Enhanced by Surface Activity, Calcium, and Protein Interactions. ACS Earth and Space Chemistry, 2019, 3, 2539-2548.	2.7	27
27	Reduced Extracellular Matrix Stiffness Prompts SH-SY5Y Cell Softening and Actin Turnover To Selectively Increase Al²(1–42) Endocytosis. ACS Chemical Neuroscience, 2019, 10, 1284-1293.	3.5	16
28	Lab on a tip: atomic force microscopy – photothermal infrared spectroscopy of atmospherically relevant organic/inorganic aerosol particles in the nanometer to micrometer size range. Analyst, The, 2018, 143, 2765-2774.	3.5	25
29	Directly Probing the Phase States and Surface Tension of Individual Submicrometer Particles Using Atomic Force Microscopy. ACS Symposium Series, 2018, , 245-259.	0.5	4
30	Mechanosensitive Endocytosis of High-Stiffness, Submicron Microgels in Macrophage and Hepatocarcinoma Cell Lines. ACS Applied Bio Materials, 2018, 1, 1254-1265.	4.6	12
31	Molecular Diversity of Sea Spray Aerosol Particles: Impact of Ocean Biology on Particle Composition and Hygroscopicity. CheM, 2017, 2, 655-667.	11.7	111
32	Direct Surface Tension Measurements of Individual Sub-Micrometer Particles Using Atomic Force Microscopy. Journal of Physical Chemistry A, 2017, 121, 8296-8305.	2.5	42
33	Solid, Semisolid, and Liquid Phase States of Individual Submicrometer Particles Directly Probed Using Atomic Force Microscopy. Analytical Chemistry, 2017, 89, 12720-12726.	6.5	38
34	Linking hygroscopicity and the surface microstructure of model inorganic salts, simple and complex carbohydrates, and authentic sea spray aerosol particles. Physical Chemistry Chemical Physics, 2017, 19, 21101-21111.	2.8	65
35	Core and surface microgel mechanics are differentially sensitive to alternative crosslinking concentrations. Soft Matter, 2017, 13, 5684-5695.	2.7	23
36	Synthesis, Optimization, and Performance Demonstration of Electrospun Carbon Nanofiber–Carbon Nanotube Composite Sorbents for Point-of-Use Water Treatment. ACS Applied Materials & Interfaces, 2016, 8, 11431-11440.	8.0	54

ALEXEI V TIVANSKI

#	Article	IF	CITATIONS
37	Enrichment of Saccharides and Divalent Cations in Sea Spray Aerosol During Two Phytoplankton Blooms. Environmental Science & Technology, 2016, 50, 11511-11520.	10.0	90
38	Quantifying the Hygroscopic Growth of Individual Submicrometer Particles with Atomic Force Microscopy. Analytical Chemistry, 2016, 88, 3647-3654.	6.5	50
39	Humidity-dependent surface tension measurements of individual inorganic and organic submicrometre liquid particles. Chemical Science, 2015, 6, 3242-3247.	7.4	56
40	Size Matters in the Water Uptake and Hygroscopic Growth of Atmospherically Relevant Multicomponent Aerosol Particles. Journal of Physical Chemistry A, 2015, 119, 4489-4497.	2.5	110
41	Determination of concentration and activity of immobilized enzymes. Analytical Biochemistry, 2015, 484, 169-172.	2.4	9
42	The Impact of Aerosol Particle Mixing State on the Hygroscopicity of Sea Spray Aerosol. ACS Central Science, 2015, 1, 132-141.	11.3	64
43	A calibration curve for immobilized dihydrofolate reductase activity assay. Data in Brief, 2015, 4, 19-21.	1.0	5
44	Mechanical Properties of a Series of Macro- and Nanodimensional Organic Cocrystals Correlate with Atomic Polarizability. Journal of the American Chemical Society, 2015, 137, 12768-12771.	13.7	48
45	Substrate-Deposited Sea Spray Aerosol Particles: Influence of Analytical Method, Substrate, and Storage Conditions on Particle Size, Phase, and Morphology. Environmental Science & Technology, 2015, 49, 13447-13453.	10.0	35
46	Role of Organic Coatings in Regulating N ₂ O ₅ Reactive Uptake to Sea Spray Aerosol. Journal of Physical Chemistry A, 2015, 119, 11683-11692.	2.5	34
47	Nanocrystals of a Metal–Organic Complex Exhibit Remarkably High Conductivity that Increases in a Single-Crystal-to-Single-Crystal Transformation. Journal of the American Chemical Society, 2014, 136, 6778-6781.	13.7	92
48	Hygroscopic Properties of Internally Mixed Particles Composed of NaCl and Water-Soluble Organic Acids. Environmental Science & Technology, 2014, 48, 2234-2241.	10.0	88
49	From co-crystals to functional thin films: photolithography using [2+2] photodimerization. Chemical Science, 2013, 4, 4304.	7.4	37
50	Field and laboratory studies of reactions between atmospheric water soluble organic acids and inorganic particles. , 2013, , .		0
51	Heterogeneous ice nucleation and water uptake by field ollected atmospheric particles below 273 K. Journal of Geophysical Research, 2012, 117, .	3.3	52
52	Self-Assembled Enzymatic Monolayer Directly Bound to a Gold Surface: Activity and Molecular Recognition Force Spectroscopy Studies. Journal of the American Chemical Society, 2011, 133, 13284-13287.	13.7	13
53	Spectroscopic Evidence of Ketoâ^'Enol Tautomerism in Deliquesced Malonic Acid Particles. Journal of Physical Chemistry A, 2011, 115, 4373-4380.	2.5	59
54	Thixotropic Hydrogel Derived from a Product of an Organic Solid-State Synthesis: Properties and Densities of Metalâ ''Organic Nanoparticles. Journal of the American Chemical Society, 2011, 133, 3365-3371.	13.7	91

ALEXEI V TIVANSKI

#	Article	IF	CITATIONS
55	Semiconducting Organic Assemblies Prepared from Tetraphenylethylene Tetracarboxylic Acid and Bis(pyridine)s via Charge-Assisted Hydrogen Bonding. Journal of the American Chemical Society, 2011, 133, 8490-8493.	13.7	76
56	Softening and Hardening of Macro―and Nano‣ized Organic Cocrystals in a Singleâ€Crystal Transformation. Angewandte Chemie - International Edition, 2011, 50, 8642-8646.	13.8	92
57	Microscopic characterization of carbonaceous aerosol particle aging in the outflow from Mexico City. Atmospheric Chemistry and Physics, 2010, 10, 961-976.	4.9	85
58	Atomic force microscopy study of photoreversible nanoscale surface relief grating patterns on side chain dendritic polyester thin films. Colloids and Surfaces A: Physicochemical and Engineering Aspects, 2010, 360, 167-174.	4.7	5
59	Quantifying reaction spread and x-ray exposure sensitivity in hydrogen silsesquioxane latent resist patterns with x-ray spectromicroscopy. Journal of Vacuum Science and Technology B:Nanotechnology and Microelectronics, 2010, 28, 1304-1313.	1.2	6
60	Nighttime chemical evolution of aerosol and trace gases in a power plant plume: Implications for secondary organic nitrate and organosulfate aerosol formation, NO ₃ radical chemistry, and N ₂ O ₅ heterogeneous hydrolysis. Journal of Geophysical Research, 2010, 115, .	3.3	67
61	Hygroscopic Behavior of Individual Submicrometer Particles Studied by X-ray Spectromicroscopy. Analytical Chemistry, 2010, 82, 9289-9298.	6.5	38
62	Electromechanical Properties of Self-Assembled Monolayers of Tetrathiafulvalene Derivatives Studied by Conducting Probe Atomic Force Microscopy. Journal of Physical Chemistry C, 2010, 114, 4429-4435.	3.1	22
63	Chemical speciation of sulfur in marine cloud droplets and particles: Analysis of individual particles from the marine boundary layer over the California current. Journal of Geophysical Research, 2008, 113, .	3.3	89
64	Investigation of the Assembly of Comb Block Copolymers in the Solid State. Macromolecules, 2008, 41, 7687-7694.	4.8	58
65	Characterization of Aerosols Containing Zn, Pb, and Cl from an Industrial Region of Mexico City. Environmental Science & Technology, 2008, 42, 7091-7097.	10.0	143
66	Pressure-Induced Restructuring of a Monolayer Film Nanojunction Produces Threshold and Power Law Conduction. Langmuir, 2008, 24, 2288-2293.	3.5	4
67	Particle formation from pulsed laser irradiation of soot aggregates studied with a scanning mobility particle sizer, a transmission electron microscope, and a scanning transmission x-ray microscope. Applied Optics, 2007, 46, 959.	2.1	62
68	Chemical bonding and structure of black carbon reference materials and individual carbonaceous atmospheric aerosols. Journal of Aerosol Science, 2007, 38, 573-591.	3.8	97
69	Oxygenated Interface on Biomass Burn Tar Balls Determined by Single Particle Scanning Transmission X-ray Microscopy. Journal of Physical Chemistry A, 2007, 111, 5448-5458.	2.5	94
70	Scanning x-ray microscopy investigations into the electron-beam exposure mechanism of hydrogen silsesquioxane resists. Journal of Vacuum Science & Technology B, 2006, 24, 3048.	1.3	12
71	Ferrocenylundecanethiol Self-Assembled Monolayer Charging Correlates with Negative Differential Resistance Measured by Conducting Probe Atomic Force Microscopy. Journal of the American Chemical Society, 2005, 127, 7647-7653.	13.7	42
72	Conjugated Thiol Linker for Enhanced Electrical Conduction of Goldâ^'Molecule Contacts. Journal of Physical Chemistry B, 2005, 109, 5398-5402.	2.6	77

#	Article	IF	CITATIONS
73	The role of adhesion forces in nanoscale measurements of the conductive properties of organic surfaces using conductive probe AFM. , 2004, , .		0
74	Adhesion Forces in Conducting Probe Atomic Force Microscopy. Langmuir, 2003, 19, 1929-1934.	3.5	30
75	Vibrational Mode Coupling to Ultrafast Electron Transfer in [(CN)5OsCNRu(NH3)5]-Studied by Femtosecond Infrared Spectroscopy. Journal of Physical Chemistry A, 2003, 107, 9051-9058.	2.5	19